The Spanwise Distributions of Characteristic Values near a Side-Wall of a Circular Cylinder with Tangential Blowing (Effect of Angular Location of a Blowing Slot)

by

Ryoji WAKA* and Fumio YOSHINO*

* Department of Mechanical Engineering

(Received August 2, 1984)

The experiment was carried out to understand the effect of the angular location of a blowing slot on the spanwise distributions of various characteristic values near the side-wall of a circular cylinder with tangential blowing. The distributions of the characteristic values near the side-wall are much influenced, and the range of the side-wall-effects is altered, by varying the location of the slot. When the shape of the slot like a knife edge is used, the range of the side-wall-effects becomes narrower as the angular location of the blowing slot is more downstream.

1. Introduction

Up to date, the authors have carried out the synthetic investigations on a circular cylinder with tangential blowing including the visualization of the flow itself inside the test section and those on various characteristic values such as aerodynamic coefficients.[1] ~ [3]

According to these, a roll up of a strong vortex took place near the side-wall in a case of a circular cylinder even if the experiment was carried out on a two-dimentional model. Hence, there is a wide range near the side-wall in which the approximation of the two-dimensional flow no longer holds, and the effect of induced velocity is not negligible even at the mid-span where the two-dimensional approximation is applicable. This is an important problem for a circular cylinder in particular, since it is difficult to make an aspect ratio of the cylinder with blowing large enough.

Now, the range of the side-wall-effects is defined as the semi-span minus the spanwise distance from the mid-span to the point from which toward the side-wall the two-dimensional approximation is not applicable. Then it is important to understand not only the spanwise distribution of induced angle of attack but also the range of the side-wall-effects. However, there are only few investigations on the circular cylinder with tangential blowing[4] ~ [8] and even fewer investigations on the flow near the side-wall so far. This may have been caused by complexity of this problem and experimental difficulty due to numerous parameters.

From the viewpoints mentioned above, the authors already published a paper on the range of the side-wall-effects and the spanwise distribution of induced angle of attack calculated theoretically and so on.[1] After that, the experiment with the angular location of the blowing slot as a parameter was carried out, since the investifation on the side-wall-effects was yet insufficient.

In this report, the effects of the slot location on various characteristic values near the side-wall are discussed on the basis of known facts in the previous reports.

2. Nomenclature

C_d : section drag coefficient
C_l : section lift coefficient
C_{ln} : lift coefficient normalized by C_l at the mid-span
C_p : pressure coefficient
C_{pb} : base pressure coeffidient
C_μ : momentum coefficient of the blowing jet [=(momentum of jet per unit span)/$(1/2)\rho U_\infty^2 D$]
D : diameter of the circular cylinder
Re : Reynolds number ($= U_\infty D/\nu$)

U_∞ : velocity of a uniform flow
y_w : coordinate taken to the port direction from the starboard side-wall
η_w : $= y_w / D$ ($\eta_w = -4$ at the mid-span)
θ : angle measured clockwise from the leading edge of the cylinder
θ_j : angular location of the slot
θ_u : angular position of the separation point on the upper surface of the cylinder
ν : kinematic viscosity of air
ρ : dencity of air
Subscript
0 : value at the mid-span

3. Experimental Apparatus and Method

3-1 Experimental apparatus

The experimental apparatus used for the present investigation is the same one[1] as already described except for a height of the slot.

Figure 1 shows a cross section of the model cylinder. A hollow cylinder with an outer diameter of 100 mm and a small cylinder with a diameter of 25 mm form a blowing slot with a constant height of 0.58 mm across the whole span. The outer surface of the cylinder is chromium-plated and the static pressure holes of 335 in total are circumferentially distributed at ten spanwise sections.

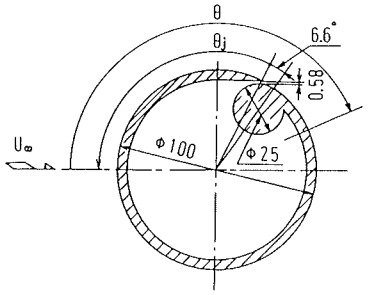

Fig.1 Cross section of the model cylinder

Figure 2 shows a test section of the wind tunnel. The model cylinder is mounted at the center of the test section and passes through two partition-plates of 10 mm thick inside the test section (hereinafter referred to as "side-wall") and the tunnel walls.

The shape of the slot of the cylinder-side-wall juncture used in this experiment is illus-

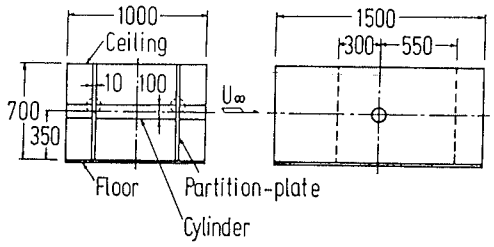

Fig.2 Test section of the wind tunnel

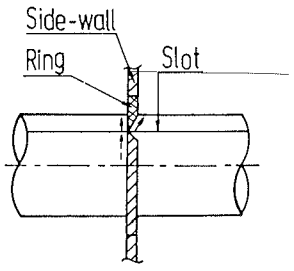

Fig.3 Shape of the slot .

trated in the dotted circles in Fig.3. It is called "Edge Type" here and abbreviated as "ED".

3-2 Experimental method

The experiment was carried out by varying θ_j and C_μ under the conditions of constant Re of 2.1×10^5, constant aspect ratio of 8 and a fixed shape of the slot of ED shown in Fig. 3. θ_j was varied to five different locations of $\theta_j = 50^\circ$, 70°, 90°, 110° and 120°.

The experiment for each θ_j is divided into two parts one of which is a case of varying C_μ arbitrarily, the other of which is a case of adjusting C_μ so as to give the same value of C_{10} at each θ_j. Two desired values of C_{10} were used aiming at about 3.6 and 6.2. The circumferential static pressure distributions were measured with a multitube manometer for all the cases mentioned above.

4. Experimental Results

Figures 4(a) and (b) show the spanwise distributions of θ_u. In the figures from Fig. 4 to 6, (a) indicates the case of varying C_μ arbitrarily for each θ_j and (b) the case of adjusting C_μ so as to give the same value of C_{10} at each θ_j.

According to Fig. 4(a), θ_u gradually increases with an approach to the side-wall and after taking a maximum value, θ_u rapidly decreases. When θ_j is fixed and C_μ increases, θ_u increases over the whole span with the increase of C_μ and in general the larger θ_j is, the larger θ_u is. Since θ_u has a minimum value at the side-wall ($\eta_w=0$), it is found that the separation of flow first occures there. The spanwise position of the maximum point scarcely moves by the change of C_μ but moves toward the side-wall as θ_j increases.

In the case of the same value of C_{10} (Fig. 4(b)), the spanwise distribution is considerably different near the side-wall among θ_j's used here although the values of C_{10} are nearly constant irrespective of the values of θ_j. Namely, in spite of small C_μ, the larger θ_j is, the larger the maximum value of θ_u is. Moreover, as θ_j increases, the spanwise position of the maximum point moves toward the side-wall.

Figures 5(a) and (b) show the spanwise distributions of C_{pb}. Now, C_{pb} is defined as a mean value of C_p's at the upper and lower separation points. In Fig. 5(a), C_{pb} gradually decreases with an approach to the side-wall and after taking a minimum value near the side-wall, C_{pb} rapidly increases. On the other hand, C_{pb0} increases with the increase of C_μ for all θ_j's. When $\theta_j \leqq 70^\circ$, the minimum point is not clearly seen near the side-wall even when C_μ is relatively large and C_{pb} merely decreases a little toward the side-wall. The difference in the spanwise distributions of C_{pb} among different C_μ's is also little. When $\theta_j=90^\circ$, if C_μ is large enough, the minimum point of C_{pb} is clearly seen. As C_μ increases, both C_{pb}'s near the side-wall and at the minimum point decrease. When $\theta_j \geqq 110^\circ$, the minimum point of C_{pb} appears near the side-wall even when C_μ is small enough,

and in particular when C_μ increases beyond the value of about 0.1, the minimum value abruptly drops. The spanwise position of the minimum point is nearly independent of C_μ, depends on θ_j only, and it moves toward the side-wall with the increase of θ_j.

In Fig. 5(b), the values of C_{pb0} are nearly independent of θ_j for both cases of $C_{10}\fallingdotseq 3.6$ and 6.2. When $C_{10}\fallingdotseq 3.6$, the distribution curve of C_{pb} is relatively flat and C_{pb} gradually decreases a little near the side-wall. The value of C_{pb} near the side-wall in the case of $\theta_j \geqq 110^\circ$ is a little greater compared with that of $\theta_j \leqq 90^\circ$. When $C_{10}\fallingdotseq 6.2$, however, C_{pb} rapidly decreases near the side-wall and the minimum point is clearly seen there. In particular, the decrease of C_{pb} is remarkable in the case of $\theta_j \geqq 90^\circ$ compared with that of $\theta_j = 70^\circ$.

Figures 6(a) and (b) show the spanwise distributions of C_d. In Fig. 6(a), C_d gradually increases with an approach to the side-wall and after taking a maximum value, C_d rapidly decreases. As C_μ increases, both C_{d0} and the maximum value of C_d increase but C_d at the side-wall decreases on the contrary. C_{d0} tends to

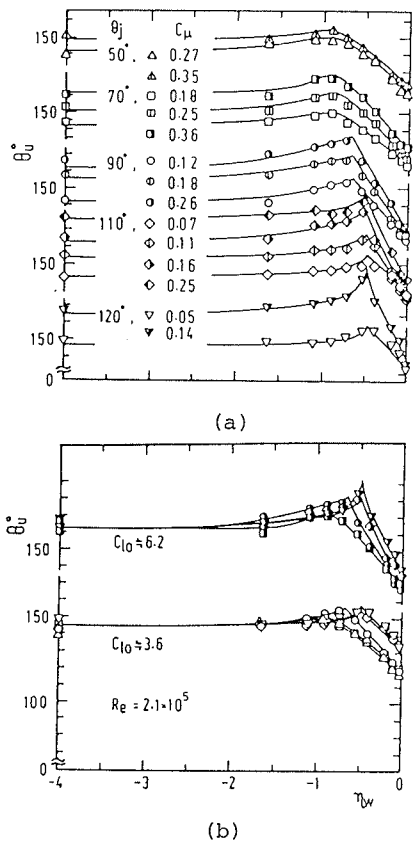

Fig.4 Spanwise distributions of θ_u

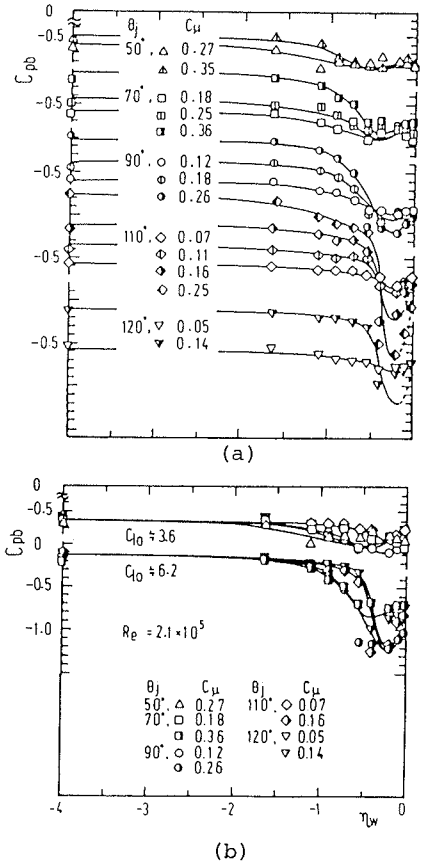

Fig.5 Spanwise distributions of C_{pb}

increase a little with the increase of C_μ and there are maximum values in the spanwise distributions of each θ_j which increase with C_μ. The distribution curve becomes sharper near the maximum point and this tendency becomes strong when C_μ increases beyond the value of about 0.1. Moreover, the spanwise position of the maximum point is independent of C_μ and moves toward the side-wall with the increase of θ_j.

In Fig. 6(b), when $C_{l0}\fallingdotseq 3.6$, the spanwise distribution curve of C_d is relatively smooth without a clear peak for each θ_j. When $\theta_j \geqq 110^\circ$ the distribution curve near the side-wall is sharper compared with that of $\theta_j \leqq 70^\circ$, and the distribution curve of $\theta_j = 90^\circ$ lies in between those of $\theta_j \geqq 110^\circ$ and $\theta_j \leqq 70^\circ$. This tendency described here is more emphasized in the case of $C_{l0}\fallingdotseq 6.2$. When $C_{l0}\fallingdotseq 6.2$, the distribution curve near the peak becomes particuraly steep in the case of $\theta_j \geqq 110^\circ$. For $\theta_j = 90^\circ$, C_d becomes larger over the wide range of the span. The spanwise positions of the maximum point of C_d moves toward the side-wall with the increase of θ_j for all the cases of C_{l0}. Moreover, the value of C_d is less than that of C_{d0} very near the side-wall. However, any systematic dependence on θ_j is not observed in C_{d0}.

Now, the spanwise distance from the side-wall to the point of the extremum for each characteristic value, η_w, is tabulated in Table I, when θ_j is varied.

Figure 7 shows the spanwise distributions of C_{ln}. The experimental results

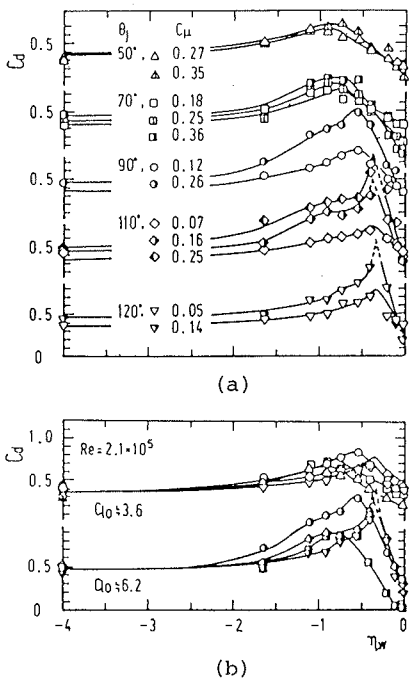

Fig.6 Spanwise distributions of C_d

Table I Spanwise positions of the extremum of characteristic values

θ_j°	50	70	90	110	120
θ_u	-0.98	-0.92	-0.65	-0.50	-0.48
C_{pb}	-0.52	-0.46	-0.28	-0.22	-0.18
C_d	-0.88	-0.80	-0.60	-0.38	-0.34
Vortex	-0.61	-0.52	-0.40	-0.25	-0.22

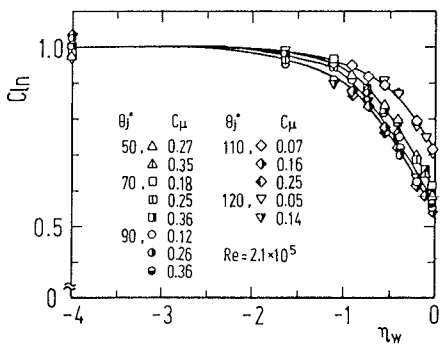

Fig.7 Spanwise distributions of C_{ln}

of not only the cases of adjusted C_μ to give equal C_{10} but also the cases of arbitrary C_μ are shown in this figure. If C_{10} is large enough, the distribution of C_{1n} is uniquely determined by θ_j independently of C_μ within the range of experimental error. Hence, it is found that the spanwise distribution of C_1 is independent of C_μ and is similar except for the case of both $\theta_j \geqq 110^\circ$ and $C_{10} \fallingdotseq 3.6$.

Figure 8 shows the static pressure distributions on the cylinder surface for the cases of $\theta_j = 70^\circ$, 90° and 120° at $C_{10} \fallingdotseq 6.2$. This figure is a developed surface of the circular cylinder to give clearer image of the separated region near the side-wall. There is a particularly low pressure part in the separated region near the side-wall. According to the observation of the limiting stream lines on the cylinder surface, the spanwise position of this lower pressure part is in accord with that of a vortex shed directly from the cylinder surface and swallowed up into the center of the trailing vortex. As θ_j increases, the vortex moves toward the side-wall and the pressure gradient near the vortex becomes steeper. Hence, the two-dimensional region becomes wider in the left side of the vortex by the rightward movement of that with the increase of θ_j.

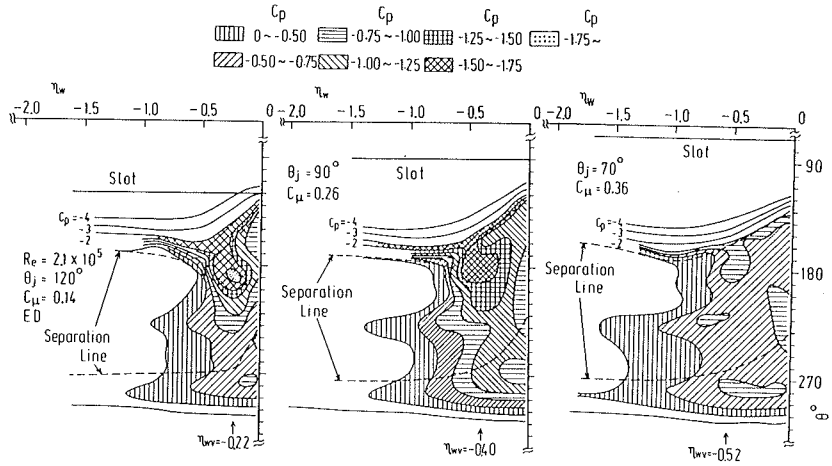

Fig.8 Static pressure distributions on the cylinder surface

5. Discussion

5-1 The range of the side-wall-effects

The spanwise range of the side-wall-effects was defined as the range near the side-wall in which the flow around the cylinder was no longer approximated as quasi-two-dimensional. Then, it is expected that the range of the side-wall-effects is closely related to the spanwise position of the rolled-up-shed vortex near the side-wall. Since the position of the vortex moves toward the side-wall

with the increase of θ_j as shown in Table I, the range of the side-wall-effects will become narrower with the increase of θ_j. The method determining this range was already described in references of (1) and (3). The ranges of the side-wall-effects obtained by this method for various θ_j's are tublated in Table II. As mentioned above, this range is also altered according to the variation of the spanwise position of the vortex and it becomes narrower with the increase of θ_j. Then, the slot ought to be located as downstream as possible in order to obtain the two-dimensional range in the experiment as wide as possible.

Table II Range of the side-wall-effects

θ_j°	η_w
50	-1.86
70	-1.45
90	-1.30
110	-1.24
120	-1.20

5-2 The relation between the slot position and the range of the side-wall-effects

As mentioned in the preceding section, the range of the side-wall-effects is closely related to the spanwise position of the vortex, η_{wv}.

Figure 9 shows the relation between η_{wv} and θ_j obtained from Table I. η_{wv} nearly proportional to θ_j, and since this relation is independent of C_μ, η_{wv} should be determined by θ_j only.

Next, the relation between $(C_{l0}-C_{lw})$ and $(C_{pb0}-C_{pbv})^{1/2}$ is shown in Fig. 10. Now, C_{pbv} is the minimum value in the spanwise distribution of C_{pb} and is to be regarded as an approximate value of C_{pb} at the vortex core on the cylinder surface. C_{lw} is the value of C_l at the side-wall ($\eta_w=0$). $(C_{pb0}-C_{pbv})^{1/2}$ is proportional to $(C_{l0}-C_{lw})$. Since $(C_{l0}-C_{lw})$ is proportional to the total amount of the trailing vortex shed from the cylinder between the mid-span and the side-wall (hereinafter referred to as "strength of the trailing vortex"), $(C_{pb0}-C_{pbv})^{1/2}$

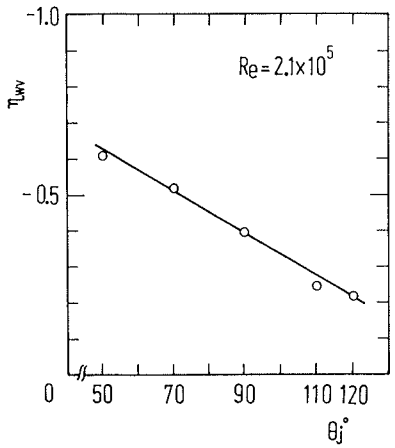

Fig.9 Relation between η_{wv} and θ_j

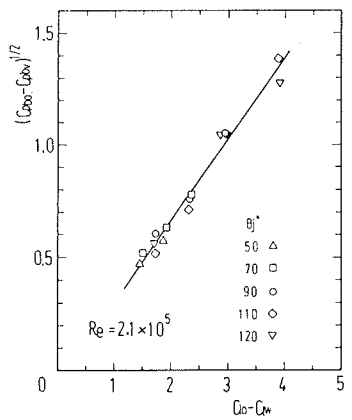

Fig.10 Relation between $(C_{l0}-C_{lw})$ and $(C_{pb0}-C_{pbv})^{1/2}$

ought to be proportional to the strength of the trailing vortex.

On the other hand, $(C_{pb0}-C_{pbv})^{1/2}$ is considered to be approximately proportional to the strength of the vortex core (vortex tube), because it indicates the square root of pressure difference between the pressure of vortex core and that in the separated region distant enough from the vortex core. Therefore, if only θ_j increases under constant $(C_{10}-C_{1w})$, the vortex core should move toward the side-wall keeping its strength constant, since the spanwise position of vortex, η_{wv}, is determined by θ_j only independently of C_μ (Fig. 9). Now, even though C_μ increases under the fixed θ_j, both the values of η_{wv} and the range of the side-wall-effects are unchanged as described earlier but the value of $(C_{10}-C_{1w})$ increases (Fig. 7). Since $(C_{pb0}-C_{pbv})^{1/2}$ increases proportionally to $(C_{10}-C_{1w})$, the vortex core little changes the size but increases its strength in this case. It is concluded from these discussions that the spanwise position and the strength of the vortex core are altered only by θ_j and $(C_{10}-C_{1w})$ respectively, keeping its size constant. Considering like this, it is found that the larger decrease of the minimum value of C_{pbv} in the case of $\theta_j \geqq 90^\circ$ than that in the case of $\theta_j=70^\circ$ (Fig. 5(a)) results from the increase in the strength of the vortex core due to the increase of $(C_{10}-C_{1w})$ when only θ_j is varied under the condition of constant C_{10}.

6. Conclusions

Experiment was carried out on the spanwise distributions of various characteristic values of the circular cylinder with tangential blowing for various locations of the slot and jet intensities. The conclusions from all of these are as follows;

(1) The range of the side-wall-effects is obtained for each location of the slot as shown in Table II.

(2) The range of the side-wall-effects becomes narrower with the increase of θ_j and is independent of C_μ.

(3) If θ_j is fixed, the spanwise distribution of C_1 is similar except for the case that C_μ is small and $\theta_j \geqq 110^\circ$

(4) The strength of the vortex core is proportional to that of the trailing vortex.

References

(1) Yoshino, F., et al., Bulletin of the JSME, vol.24, No.192 (1981-6), p.926.
(2) Waka, R., et al., Int. Sympo. on Flow Visualization, Bochum (1980), p.528.
(3) Waka, R., et al., Bulletin of the JSME, vol.26, No.215 (1983-5), p.755.
(4) Dunham, J., J.Fluid Mech., vol.33, part 3 (1968-9), p.495.

(5) Sato, M. and Matsuoka, K., Trans. Japan Soc. Mech. Engrs. (in Japanese), vol.36, No.289 (1970-9), p.1493.
(6) Furuya, Y. and Yoshino, F., Trans. Japan Soc. Mech. Engrs. (in Japanese), vol.41, No.341 (i975-1), p.170.
(7) Ueda, S. and Tanaka, H., Trans. Japan Soc. Mech. Engrs. (in Japanese), vol.41, No.350 (1975-10), p.2853.
(8) Furuya, Y. and Yoshino, F., Trans. Japan Soc. Mech. Engrs. (in Japanese), vol.42, No.358 (1976-6), p.1830.